# Chapter 8
# Watershed Scale Physically Based Water Flow, Sediment and Nutrient Dynamic Modeling System

**Billy E. Johnson, Zhonglong Zhang and Charles W. Downer**

**Abstract** Non-point source (NPS) runoff of pollutants is viewed as one of the most important factors causing impaired water quality in freshwater and estuarine ecosystems and has been addressed as a national priority since the passage of the Clean Water Act. To control NPS pollution, state and federal agencies developed a variety of programs that rely heavily on the use of watershed management in minimizing riverine and receiving water pollution. Watershed models have become critical tools in support of watershed management. Lumped, empirical models such as HSPF do not account for spatial heterogeneity within subwatersheds and the simulations of the actual processes are greatly simplified. This chapter describes a distributed water flow, sediment and nutrient dynamic modeling system developed at U.S. Army Engineer Research and Development Center. The model simulates detailed water flow, soil erosion, nitrogen (N) and phosphorus (P) cycling at the watershed scale and computes sediment transport across the landscape, nutrient kinetic fluxes for N and P species. The model consists of three distinct parts: (1) watershed hydrology, (2) soil erosion and sediment transport, and (3) nitrogen and phosphorus transport and cycling. The integrated watershed model was tested and validated on two watersheds in Wisconsin (French Run and Upper Eau Galle Watersheds). The model performed well in predicting runoff, sediment, nitrogen and phosphorus. This chapter presents the model development and validation studies currently underway in Wisconsin.

B. E. Johnson (✉)
Environmental Laboratory, U.S. Army Engineer Research and Development Center, 3909 Halls Ferry Rd, Vicksburg, MS 39180, USA
e-mail: Billy.E.Johnson@usace.army.mil

Z. Zhang
Badger Technical Services, U.S. Army Engineer Research and Development Center, 3909 Halls Ferry Rd, Vicksburg, MS 39180, USA

C. W. Downer
Coastal and Hydraulics Laboratory, U.S. Army Engineer Research and Development Center, 3909 Halls Ferry Rd, Vicksburg, MS 39180, USA

B. Fu and K. B. Jones (eds.), *Landscape Ecology for Sustainable Environment and Culture*, DOI: 10.1007/978-94-007-6530-6_8,

**Keywords** Watershed model · Hydrology · Sediment transport · Nonpoint source · Nutrient transformations

## 8.1 Introduction

Nutrient pollution is a leading cause of water quality impairment in lakes and estuaries and is also a significant issue in rivers (USEPA 2007). Non-point source (NPS) pollution, especially from nitrogen and phosphorus, has consistently ranked as one of the top causes of degradation in some U.S. waters. Nutrient problems can exhibit themselves locally or much further downstream leading to degraded estuaries, lakes and reservoirs, and to hypoxic zones where fish and aquatic life can no longer survive. The growing concern about the environmental impact of NPSs has enhanced a "watershed approach" to reduce NPS pollution and coordinate the management of water resources. The concept of this watershed approach is based on multi-purpose, multi-objective management, and in examining all water needs in the watershed and receiving water bodies. A watershed scale flow, sediment and water quality modeling system has been developed at U.S. Army Engineer Research and Development Center (ERDC) in support of the U.S. Army Corps of Engineers (USACE)' watershed approach.

This chapter describes the on-going watershed water quality modeling development and integration with the Gridded Surface Subsurface Hydrologic Analysis (GSSHA) model. The major chemical and physical processes influencing sediments and nutrients in the soil, overland flow and stream have been accounted for in the GSSHA. The hydrological variables required to drive the sediment and nutrient simulation were provided using the existing GSSHA model. Integrated physically based hydrologic models with sediment and nutrient transport across the landscape give more realistic descriptions of the sediment and nutrient dynamics in watersheds. This is especially important for agricultural watersheds where the sediment and nutrient play important roles and their occurrence are highly variable both in time and space. Hence, hot-spots with high contaminant loading sources can be more accurately identified and watershed management practices to reduce sediment and nutrient transport can be made more confidently.

## 8.2 Watershed Scale Water Flow and Sediment Model

The U.S. Army Corps of Engineer's Gridded Surface Subsurface Hydrologic Analysis (GSSHA) is a physically-based, distributed-parameter, structured grid, hydrologic model that simulates the hydrologic response and sediment transport of a watershed subject to given hydrometeorological inputs. The watershed is divided into grid cells that comprise a uniform finite difference grid. GSSHA is a

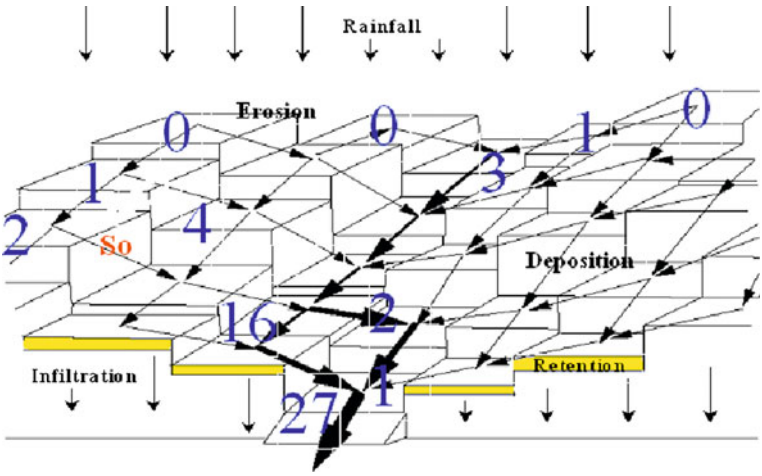


**Fig. 8.1** Topographical representation of overland flow and channel routing schemes within a watershed

reformulation and enhancement of the CASC2D (Fig. 8.1). The model incorporates 2D overland flow, 1D stream flow, 1D unsaturated flow and 2D groundwater flow components. Within GSSHA, sediment erosion and transport processes take place both on the land and within the channel. The GSSHA model employs mass conservation solutions of partial differential equations and closely links the hydrologic components to assure an overall mass balance. GSSHA had already been tested and applied for hydrologic response and sediment transport in several watersheds across the United States and achieved satisfactory results (CHL 2012). A brief introduction is given as follows however details of the GSSHA model can be found in Downer and Ogden (2004). A review of hydrologic and sediment erosion and transport process descriptions is informative to illustrate the physics behind individual process representations and specific to those needed to drive full nitrogen and phosphorus cycling at the watershed scale.

### *8.2.1 Hydrologic Simulation*

The modeling of hydrologic processes begins with rainfall being added to the watershed, some of which is intercepted by the canopy cover, evapotranspirated or infiltrated. Hydrologic processes that can be simulated and the methods used to approximate the processes with the GSSHA model are listed in Table 8.1.

GSSHA uses two-step, finite-volume schemes to route water for both 2D overland flow and 1D channel flow where flows are computed based on heads and volumes are updated based on the computed flows. Several modifications were made to both the GSSHA channel routing and the overland flow routing schemes

**Table 8.1** Processes and approximation techniques in the GSSHA model

| Process | Approximation |
|---|---|
| Precipitation distribution | Thiessen polygons (nearest neighbor) Inverse distance-squared weighting |
| Snowfall accumulation and melting | Energy balance |
| Precipitation interception | Empirical two parameter |
| Overland water retention | Specified depth |
| Infiltration | Green and Ampt (GA) Multi-layered GA Green and Ampt with Redistribution (GAR) Richard's equation (RE) |
| Overland flow routing | 2-D diffusive wave |
| Channel routing | 1-D diffusive wave, 1-D dynamic wave |
| Evapo-transpiration | Deardorff Penman-Monteith with seasonal canopy resistance |
| Soil moisture in the vadose zone | Bucket model RE |
| Lateral groundwater flow | 2-D vertically averaged |
| Stream/groundwater interaction | Darcy's law |
| Exfiltration | Darcy's law |

to improve stability, and allow interaction between the surface and subsurface components of the model. The combination of improvements in the stability of the overland and channel routing schemes has allowed significant increases in model computational time steps over previous versions.

#### 8.2.1.1 Overland Flow Routing

Water flow across the land surface is shallow, unsteady, and non-uniform. This flow regime can be described by the Saint-Venant equations which are derived from physical laws regarding the conservation of mass and momentum. Overland flow routing in GSSHA employs the 2D diffusive wave equation, which allows for backwater and reverse flow conditions. The 2D (vertically integrated) continuity equation for gradually-varied flow over a plane in rectangular (x, y) coordinates is (Julien et al. 1995):

$$\frac{\partial h}{\partial t} + \frac{\partial q_x}{\partial x} + \frac{\partial q_y}{\partial y} = i_e \tag{8.1}$$

where $h$ = surface water depth [L], $q_x$, $q_y$ = unit discharge in the x- or y-direction = $Q_x/B_x$, $Q_y/B_y$ [$L^2$/T], $Q_x$, $Q_y$ = flow in the x- or y-direction [$L^3$/T], $B_x$, $B_y$ = flow width in the x- or y-direction [L], $i_e$ = excess net precipitation rate [L/T].

The diffusive wave momentum equations for the x- and y-directions are written as:

$$S_{fx} = S_{0x} - \frac{\partial h}{\partial x} \tag{8.2a}$$

$$S_{fy} = S_{0y} - \frac{\partial h}{\partial y} \tag{8.2b}$$

where $S_{fx}$, $S_{fy}$ = friction slope (energy grade line) in the x- or y-direction, $S_{0x}$, $S_{0y}$ = ground surface slope in the x- or y-direction.

#### 8.2.1.2 Channel Flow Routing

Channel flow routing in GSSHA employs the 1D diffusive wave equation. The 1D (laterally and vertically integrated) continuity equation for gradually-varied flow along a channel is (Julien et al. 1995):

$$\frac{\partial A}{\partial t} + \frac{\partial Q}{\partial x} = q_l \tag{8.3}$$

where $A$ = cross sectional area of channel flow [$L^2$], $Q$ = total discharge [$L^3$/T], and $q_l$ = lateral flow into or out of the channel [$L^2$/T].

### *8.2.2 Sediment Simulation*

Sediment erosion and transport are potentially very important processes in water quality modeling. Excess sediment affects water quality directly by itself. Sediment transport also influences chemical transport and fate. Suspended sediments act as a carrier of chemicals in the watershed flow. Many chemicals sorb strongly to sediment and thus undergo settling, scour, and sedimentation. Sorption also affects a chemical's transfer and transformation rates. The amount of chemicals transported by the sediments depends on the suspended sediment concentration and the sorption coefficient. Both sediment transport rates and concentrations must be estimated in most toxic modeling studies. The sediment algorithm is included as a sub-model in GSSHA and invoked only when sediment simulation is required. The sediment sub-model is designed for estimating sediment delivery and channel transport in watersheds. It consists of four primary components: (1) sediment transport; (2) erosion; (3) deposition; and (4) bed processes (bed elevation dynamics).

#### 8.2.2.1 Sediment Transport

The sediment transport model is based on the suspended sediment mass conservation equation (advection-diffusion equation with the sink-source term describing sedimentation resuspension rate) and the equation of bottom deformation. For the overland plane in 2D, the concentration of particles in a flow is governed by conservation of mass (sediment continuity) (Julien 1998):

$$\frac{\partial C_{ss}}{dt} + \frac{\partial \hat{q}_{tx}}{\partial x} + \frac{\partial \hat{q}_{ty}}{\partial y} = \hat{J}_e - \hat{J}_d + \hat{W}_s = \hat{J}_n \tag{8.4}$$

where $C_{ss}$ = concentration of sediment particles in the flow [M/L$^3$], $\hat{q}_{tx}$, $\hat{q}_{ty}$ = total sediment transport areal flux in the x- or y-direction [M/L$^2$T], $\hat{J}_e$ = sediment erosion volumetric flux [M/L$^3$T], $\hat{J}_d$ = sediment deposition volumetric flux [M/L$^3$T], $\hat{W}_s$ = sediment point source/sink volumetric flux [M/L$^3$T], $\hat{J}_n$ = net sediment transport volumetric flux [M/L$^3$T].

The total sediment transport flux in any direction has three components, advective, dispersive (mixing), and diffusive, and may be expressed as (Julien 1998):

$$\hat{q}_{tx} = u_x C_{ss} - (R_x + D)\frac{\partial C_{ss}}{\partial x} \tag{8.4a}$$

$$\hat{q}_{ty} = u_y C_{ss} - (R_y + D)\frac{\partial C_{ss}}{\partial y} \tag{8.4b}$$

where $u_x$, $u_y$ = flow (advective) velocity in the x- or y-direction [L/T], $R_x$, $R_y$ = dispersion (mixing) coefficient the x- or y-direction [L$^2$/T], $D$ = diffusion coefficient [L$^2$/T].

Note that both dispersion and diffusion are represented in forms that follow Fick's Law. However, dispersion represents a relatively rapid turbulent mixing process while diffusion represents a relatively slow a Brownian motion, random walk process (Holley 1969). In turbulent flow, dispersive fluxes are typically several orders of magnitude larger than diffusive fluxes. Further, flow conditions for intense precipitation events are usually advectively dominated as dispersive fluxes are typically one to two orders smaller than advective fluxes. As a result, both the dispersive and diffusive terms may be neglected.

Similarly, the suspended sediment transport in channels is described by the 1-D advection-diffusion equation that includes a source-sink term describing sedimentation and resuspension rates and laterally distributed inflow of sediments. The concentration of particles in flow is governed by the conservation of mass (Julien 1998):

$$\frac{\partial C_{ss}}{\partial t} + \frac{\partial \hat{q}_{tx}}{\partial x} = \hat{J}_e - \hat{J}_d + \hat{W}_s = \hat{J}_n \tag{8.5}$$

Individual terms for the channel advection-diffusion equation are identical to those defined for the overland plane. Similarly, the diffusive flux term can be neglected. The dispersive flux is expected to be larger than the corresponding term for overland flow. However, the channel dispersive flux still may be neglected relative to the channel advective flux during intense runoff events. The distributed runoff inflow to the channel and the suspended sediment concentration in the runoff are simulated by the overland component.

#### 8.2.2.2 Sediment Erosion and Deposition

In the overland plane, sediment particles can be detached from the bulk soil matrix by raindrop impact and entrained into the flow by hydraulic action when the exerted shear stress exceeds the stress required to initiate particle motion (Julien and Simons 1985). The overland erosion process is influenced by many factors including precipitation intensity and duration, runoff length, surface slope, soil characteristics, vegetative cover, exerted shear stress, and sediment particle size. In channels, sediment particles can be entrained into the flow when the exerted shear stress exceeds the stress required to initiate particle motion. For non-cohesive particles, the channel erosion process is influenced by factors such as particle size, particle density and bed forms. For cohesive particles, the erosion process is significantly influenced by inter-particle forces (such as surface charges that hold grains together and form cohesive bonds) and consolidation. The surface erosion algorithm represents the mechanisms by which sediment is eroded from hillslopes and transported to the stream or channel network. Entrainment rates may be estimated from site-specific erosion rate studies or, in general, from the difference between sediment transport capacity and advective fluxes:

$$\begin{aligned} v_r &= \frac{J_c - v_a C_{ss}}{\rho_b} \; J_c > v_a C_{ss} \\ v_r &= 0 \; J_c \le v_a C_{ss} \end{aligned} \tag{8.6}$$

where $v_r$ = resuspension (erosion) velocity [L/T], $J_c$ = sediment transport capacity areal flux [M/L$^2$/T], $v_a$ = advective (flow) velocity (in the x- or y-direction) [L/T].

The rate of sediment deposition is proportional to the sediment concentration and settling velocity. If the sediment transport capacity is lower than the sediment load, then sediment deposition occurs. The process of sediment deposition is highly selective, the settling velocity of an aggregate or particle being a function of its size, shape, and density. Coarse particles (>62 μm) are typically non-cohesive and generally have large settling velocities under quiescent conditions. Numerous empirical relationships to describe the non-cohesive particle settling velocities are available. For non-cohesive (fine sand) particles with diameters from 62 to 500 μm, the settling velocity can be computed as (Cheng 1997):

$$v_{sq} = \frac{v}{d_p}\left[\left(25 + 1.2 d_*^2\right)^{0.5} - 5\right]^{-1.5} \tag{8.7a}$$

$$d_* = d_p \left[\frac{(G-1)g}{v^2}\right]^{1/3} \tag{8.7b}$$

where $v_{sq}$ = quiescent settling velocity [L/T], $v$ = kinematic viscosity of water [L$^2$/T], and $d_*$ = dimensionless particle diameter.

Fine particles often behave in a cohesive manner. If the behavior is cohesive, flocculation may occur. Floc size and settling velocity depend on the conditions under which the floc was formed (Krishnappan 2000; Haralampides et al. 2003). As a result of turbulence and other factors, not all sediment particles settling through a column of flowing water will necessarily reach the sediment-water interface or be incorporated into the sediment bed. Beuselinck et al. (1999) suggested this process also occurs for the overland plane. When flocculation occurs, settling velocities of cohesive particles can be approximated by relationship of the form (Burban et al. 1990):

$$v_s = a \cdot d_f^m \tag{8.8a}$$

$$v_{se} = P_{dep} v_s \tag{8.8b}$$

where $v_s$ = floc settling velocity [L/T], $a$ = experimentally determined constant, $d_f$ = median floc diameter [L], $m$ = experimentally determined constant, $v_{se}$ = effective settling (deposition) velocity [L/T], and $P_{dep}$ = probability of deposition.

#### 8.2.2.3 Upper Sedimentation Processes

The upper soil and sediment bed play important roles in the transport of contaminants. Once a particle erodes, it becomes part of the flow and is transported downstream within the watershed. The fluxes of the channel erosion and sedimentation control the dynamics of the upper most contaminated layer. Particles and associated contaminants in the surficial sediments may enter deeper sediment layers by burial or be returned to the water column by scour. Whenever burial/scour occurs, particles and associated contaminants are transported through each subsurface sediment segment within a vertical stack. In response to the difference between bed form transport, erosion, and deposition fluxes, the net addition (burial) or net loss (scour) of particles from the bed causes the bed surface elevation to increase or decrease. The rise or fall of the bed surface is governed by the sediment continuity (conservation of mass) equation, various forms of which are attributed to Exner equation (Simons and Sentürk 1992). Julien (1998) presents a derivation of the bed elevation continuity equation for an elemental control volume that includes vertical and lateral (x- and y-direction) transport terms. Neglecting bed consolidation and compaction processes, and assuming that only vertical mass transport processes (erosion and deposition) occur, the sediment continuity equation for the change in elevation of the soil or sediment bed surface may be expressed as:

$$\rho_b \frac{\partial z}{dt} + v_{se} C_{ss} - v_r C_{sb} = 0 \tag{8.9}$$

where $z$ = elevation of the soil surface [L], $\rho_b$ = bulk density of soil or bed sediments [M/L$^3$], $C_{sb}$ = concentration of sediment at the bottom boundary [M/L$^3$].

## 8.3 Nutrient Cycling Simulation

There are two components to simulate water quality. The first component is for transport of reactive or nonreactive materials throughout the watershed, both insoluble and dissolved. The second component is a flexible biogeochemistry that addresses the water quality state variables and transformation processes. Water quality state variables included in GSSHA can either be transported by advection-dispersion processes or storage routing depending on the water engines. Conceptually, three hydrologic domains and associated nutrient pathways in the watershed were modeled: (1) subsurface soils, (2) overland flow, and (3) channel flow. Currently GSSHA includes: (1) subsurface soil nitrogen module, (2) subsurface soil phosphorus module, (3) soil plant dynamic module, (4) overland flow nitrogen module, (5) overland flow phosphorus module, and (6) in-stream water quality module.

### *8.3.1 Nitrogen Cycle*

The nitrogen cycle represents one of the most important nutrient cycles found in terrestrial ecosystems which includes stores of nitrogen found in the atmosphere, where it exists as a gas (mainly $N_2$) and other major stores of nitrogen including organic matter in soil and the oceans. Nitrogen in soil and water can be present in organic or inorganic forms and in either dissolved or particulate forms. The inorganic forms of nitrogen include nitrate ($NO_3^-$), nitrite ($NO_2^-$), exchangeable ammonium ($_4^+$), and fixed ammonium. The activities of humans have severely altered the nitrogen cycle. Some of the major processes involved in this alteration include: the application of nitrogen fertilizers to crops and increased deposition of nitrogen from atmospheric sources. A schematic representation of the watershed nitrogen transport and transformation processes involved in the nitrogen cycle is given in Fig. 8.2a.

#### 8.3.1.1 Nitrogen Transformations in Soils

Once in the soil, the nitrogen will transform through the processes of mineralization, immobilization, volatilization, nitrification, denitrification, plant uptake, nitrogen fixation, and sediment sorption. Most plants can only take up nitrogen in two solid forms: ammonium ion ($NH_4^+$) and the nitrate ion ($NO_3^-$). Ammonium is

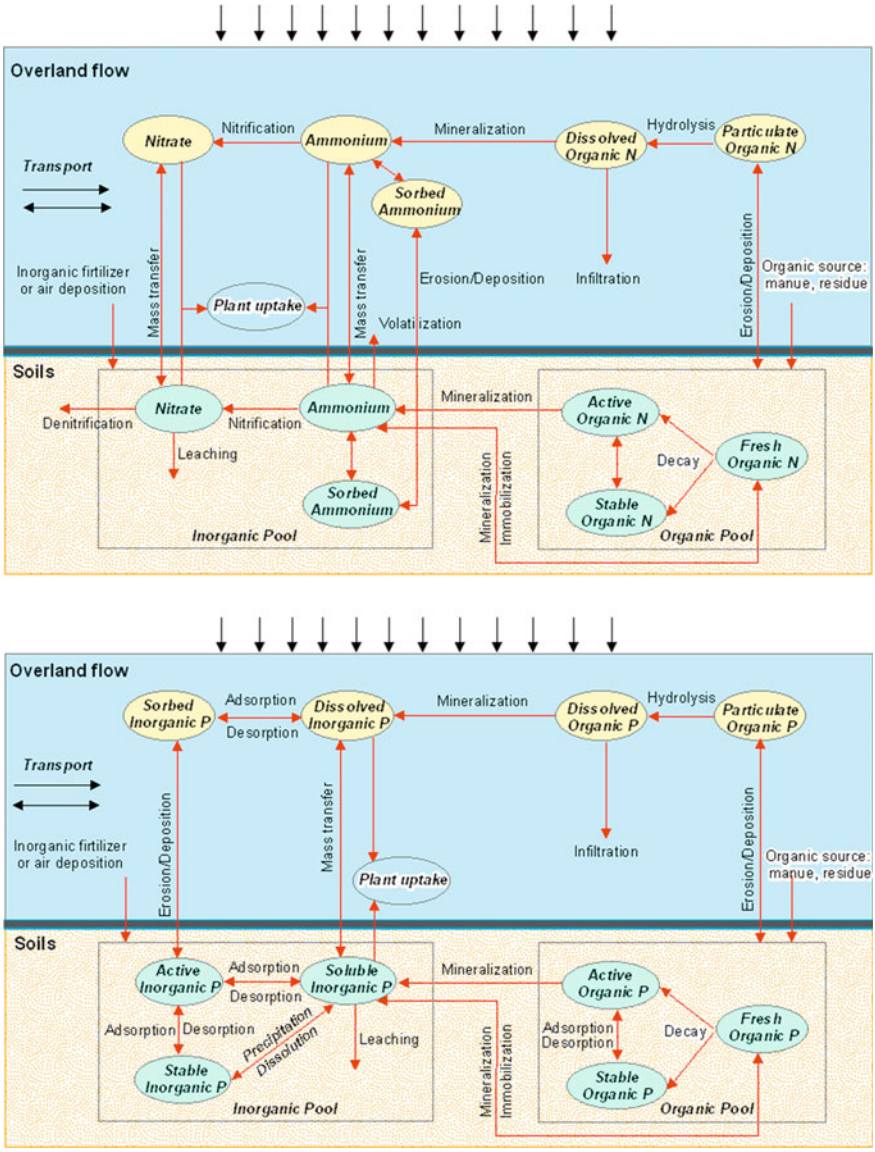


**Fig. 8.2** Simplified **a** nitrogen, and **b** phosphorus cycle in soil and water

used less by plants for uptake because in large concentrations it is extremely toxic. Mathematical models of the soil nitrogen are generally in the form of storage (pool) accounting procedures. Soil nitrogen cycling is simulated in NSM for the five pools for each of the soil layers. The mass balance equations used to describe the nitrogen cycle in soils are summarized in Table 8.2.

**Table 8.2** Mathematical expressions for soil nitrogen transformations

| N pool | N transformation equation |
|---|---|
| Fresh organic N ($orgN_{frs}$) | $\frac{d(\Delta z \cdot orgN_{frs})}{dt} = -ON_{min\|imb} - ON_{dec} - ON_{frs,e} + ON_{frs,s}$ |
| Active organic N ($orgN_{act}$) | $\frac{d(\Delta z \cdot orgN_{act})}{dt} = ON_{dec} - ON_{trn} - ON_{min} - ON_{act,e} + ON_{act,s}$ |
| Stable organic N ($orgN_{sta}$) | $\frac{d(\Delta z \cdot orgN_{sta})}{dt} = ON_{dec} + ON_{trn} - ON_{sta,e} + ON_{sta,s}$ |
| Ammonium N ($NH_4^+$) | $\frac{d(\Delta z \cdot NH_4^+)}{dt} = NH_{\min} - NH_{nit\|vol} - NH_{up} - R_{NH4,e} + NH_s$ |
| Nitrate N ($NO_3^-$) | $\frac{d(\Delta z \cdot NO_3^-)}{dt} = NH_{nit} - NO_{dnit} - NO_{up} - R_{NO3,f} - R_{NO3,e} + NO_s$ |

**Table 8.3** Mathematical expressions for overland flow nitrogen transformations

| N species | N transformation equation |
|---|---|
| Particulate organic N ($PON$) | $\frac{\partial PON_{ov}}{\partial t} = L(PON_{ov}) - k_{hn} PON_{ov}$ |
| Dissolved organic N ($DON$) | $\frac{\partial DON_{ov}}{\partial t} = L(DON_{ov}) + k_{hn} PON_{ov} - \frac{r}{h} DON_{ov} - k_{mn} DON_{ov}$ |
| Ammonium N ($NH_4^+$) | $\frac{\partial NH_{4\,ov}^+}{\partial t} = L(NH_{4\,ov}^+) + k_{mn} DON_{ov} - \frac{r}{h} NH_{4\,ov}^+ - k_{nit} NH_{4\,ov}^+ - R_{NH4,up}$ |
| Nitrate N ($NO_3^-$) | $\frac{\partial NO_{3\,ov}^-}{\partial t} = L(NO_{3\,ov}^-) + k_{nit} NH_{4\,ov}^+ - \frac{r}{h} NO_{3\,ov}^- - R_{NO3,up}$ |

#### 8.3.1.2 Nitrogen Transformations in Surface Runoff

The dominant nitrogen species in waters are dissolved inorganic nitrogen $\left(NH_4^+, NO_2^-, NO_3^-\right)$, dissolved organic nitrogen (DON), particulate organic nitrogen (PON) and particulate inorganic nitrogen (PIN) (Burt and Haycock 1993). Models may consider particulate nitrogen as a single variable, or, alternately, represent from one to many particle types or fractions. In NSM, dominant nitrogen transformation processes in surface runoff are simulated for $PON$, $DON$, $NH_4^+$, and $NO_3^-$. Transformation processes include mineralization of DON to $NH_4^+$, nitrification of $NH_4^+$, to, $NO_3^-$, plant uptake of $NH_4^+$, and, $NO_3^-$, soil mass transfer of $NH_4^+$, $NO_3^-$, and DON, sediment sorption of $NH_4^+$, and hydrolysis of PON to DON. The mass balance equations used to simulate the nitrogen cycle in surface runoff are summarized in Table 8.3.

### *8.3.2 Phosphorus Cycle*

The phosphorus cycle differs from the other major biogeochemical cycles in that it does not include a gas phase. The largest reservoir of phosphorus is in sedimentary rock. When it rains, phosphates are removed from the rocks via weathering and are distributed throughout both soils and water. Plants take up the phosphate ions from the soil. Phosphorus is not highly soluble, binding tightly to molecules in soil. Therefore it mainly reaches waters by traveling with runoff soil particles.

**Table 8.4** Mathematical expressions for soil phosphorus transformations

| P pool | P transformation equation |
|---|---|
| Fresh organic P ($orgP_{frs}$) | $\frac{d(\Delta z \cdot orgP_{frs})}{dt} = -OP_{min\|imb} - OP_{dec} - OP_{frs,e} + OP_{frs,s}$ |
| Active organic P ($orgP_{act}$) | $\frac{d(\Delta z \cdot orgP_{act})}{dt} = OP_{dec} - OP_{min} - OP_{trn} - OP_{act,e} + OP_{act,s}$ |
| Stable organic P ($orgP_{sta}$) | $\frac{d(\Delta z \cdot orgP_{sta})}{dt} = OP_{dec} + OP_{trn} - OP_{sta,e} + OP_{sta,s}$ |
| Labile (soluble) P ($P_{sol}$) | $\frac{d(\Delta z \cdot P_{sol})}{dt} = IP_{\min} - IP_{sol\|act} - IP_{up} - R_{DIP,e} + IP_s$ |
| Active inorganic P ($minP_{act}$) | $\frac{d(\Delta z \cdot minP_{act})}{dt} = IP_{sol\|act} - IP_{act\|sta} - IP_{act,e} + IP_{act,s}$ |
| Stable inorganic P ($minP_{sta}$) | $\frac{d(\Delta z \cdot minP_{sta})}{dt} = IP_{act\|sta} - IP_{sta,e} + IP_{sta,s}$ |

A schematic representation of the watershed phosphorus transport and transformation processes involved in the phosphorus cycle is given in Fig. 8.2b.

#### 8.3.2.1 Phosphorus Transformations in Soils

Phosphorus can exist in the soil as phosphate $\left(HPO_4^{-2}, \text{ or, } H_2PO_4^{-}\right)$, particulate phosphorus, organic phosphorus, or in phosphorus minerals. Many reactions and mechanisms regulate and control the composition and forms of phosphorus present in the soil. Phosphorus is generally much less mobile than nitrogen, being strongly adsorbed to soil particles as well as organic matter. Phosphorus transformations in the soil include decomposition and mineralization of organic phosphorus, immobilization of labile phosphorus, and sorption of labile phosphorus to/from soil particles, and plant uptake. Soil phosphorus cycling is simulated by NSM for the six pool state variables for each of the soil layers. The mass balance equations used to describe the phosphorus cycle in soils are summarized in Table 8.4.

#### 8.3.2.2 Phosphorus Transformations in Surface Runoff

The same process occurs within the aquatic ecosystem as for that in soils. Phosphorus is not highly soluble, binding tightly to soil particles. Therefore it mostly reaches waters by traveling with runoff soil particles. Phosphorus enters surface water primarily as particulate matter and secondarily as dissolved inorganic phosphorus (phosphate and its conjugate base forms). In NSM, dominant transformation processes are simulated for Particulate Organic Phosphorus (*POP*), Dissolved Organic Phosphorus (*DOP*), Particulate Inorganic Phosphorus (*PIP*), and Dissolved Inorganic Phosphorus (*DIP*). Transformation processes in surface runoff include mineralization of DOP to DIP, plant uptake of DIP, soil mass transfer of DIP and DOP, adsorption/desorption of DIP onto suspended sediments, and hydrolysis of POP to DOP. The mass balance equations used to simulate the phosphorus cycle in surface runoff are summarized in Table 8.5.

**Table 8.5** Mathematical expressions for overland flow phosphorus transformations

| P species | P transformation equation |
|---|---|
| Particulate organic P (*POP*) | $\frac{\partial POP_{ov}}{\partial t} = L(POP_{ov}) - k_{hp}POP_{ov}$ |
| Dissolved organic P (*DOP*) | $\frac{\partial DOP_{ov}}{\partial t} = L(DOP_{ov}) + k_{hp}POP_{ov} - \frac{r}{h}DOP_{ov} - k_{mp}DOP_{ov}$ |
| Dissolved inorganic P (*DIP*) | $\frac{\partial DIP_{ov}}{\partial t} = L(DIP_{ov}) + k_{mp}DOP_{ov} - \frac{r}{h}DIP_{ov} - R_{DIP,up}$ |

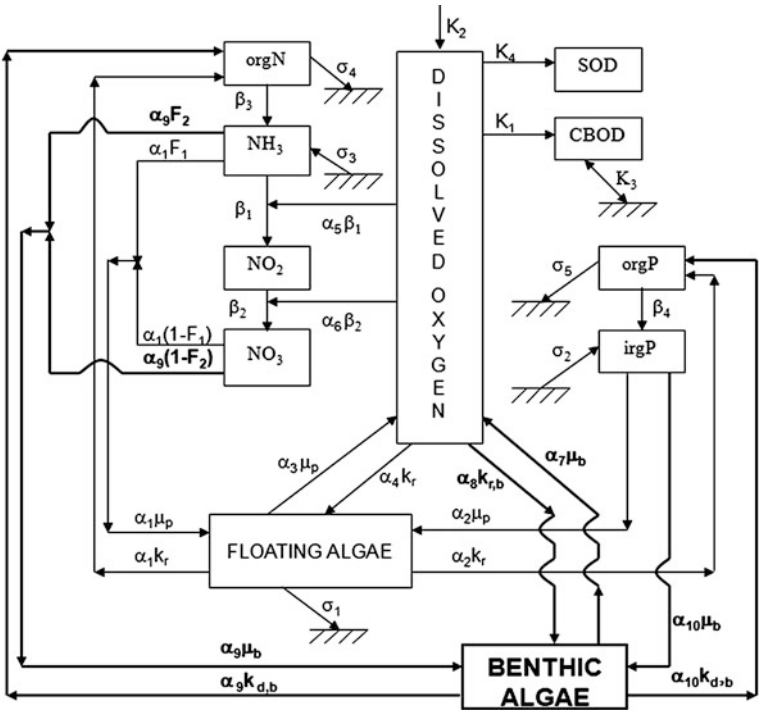


**Fig. 8.3** Schematic representation of GSSHA in-stream water quality modeling

### *8.3.3 In-Stream Water Quality*

For in-stream water quality modeling it is assumed that longitudinal and temporal changes (1D transport) are applicable. Water quality is affected in streams due to physical transport and exchange processes and biological, chemical, and biochemical kinetic processes along with changes due to benthic sediments. Currently, the in-stream water quality module includes a set of nutrient simulation kinetics. In-stream water quality kinetics computes algal biomass, organic and inorganic nitrogen and phosphorus species, CBOD and DO. The schematic representation of GSSHA in-stream water quality processes is shown Fig. 8.3.

The nutrient transport and transformation equations in the water column are summarized in Table 8.6.

**Table 8.6** Mathematical expressions for in-stream water quality processes

| Water quality variables | Transformation equation |
|---|---|
| Particulate organic N | $\frac{dON}{dt} = (\alpha_1 \cdot k_r \cdot A_p - \beta_3 \cdot ON - \sigma_4 \cdot ON) + \alpha_9 \cdot k_{db} \frac{A_b}{h} F_b$ |
| Ammonium N | $\frac{dNH4}{dt} = \left(\beta_3 \cdot ON - \beta_1 \cdot NH4 + \frac{\sigma_3}{h} - F_1 \cdot \alpha_1 \cdot \mu_p \cdot A_p\right) - F_2 \cdot \alpha_9 \cdot \mu_b \frac{A_b}{h} F_b$ |
| Nitrate N | $\frac{dNO3}{dt} = (\beta_2 \cdot NO2 - (1 - F_1)\alpha_1 \cdot \mu_p \cdot A_p) - (1 - F_2)\alpha_9 \cdot \mu_b \frac{A_b}{h} F_b$ |
| Particulate organic P | $\frac{dOP}{dt} = (\alpha_2 \cdot k_r \cdot A_p - \beta_4 \cdot OP - \sigma_5 \cdot OP) + \alpha_{10} \cdot k_{db} \frac{A_b}{h} F_b$ |
| Dissolved inorganic P | $\frac{dDIP}{dt} = \left(\beta_4 \cdot OP + \frac{\sigma_2}{h} - \alpha_2 \cdot \mu_p \cdot A_p\right) - \alpha_{10} \cdot \mu_b \frac{A_b}{h} F_b$ |
| Dissolved oxygen | $\frac{dDO}{dt} = (k_2(DO_s - DO) + (\alpha_3 \cdot \mu_p - \alpha_4 \cdot k_r)A_p - k_1 \cdot CBOD - \frac{k_4}{h} - \alpha_5 \cdot \beta_1 \cdot NH4 - \alpha_6 \cdot \beta_2 \cdot NO3) + (\alpha_7 \cdot \mu_b - \alpha_8 \cdot k_{rb})\frac{A_b}{h} F_b$ |
| Algae (phytoplankton) | $\frac{dA_p}{dt} = \left(\mu_p - k_r - \frac{\sigma_1}{h}\right)A_p$ |
| Algae (bottom algae) | $\frac{dA_b}{dt} = (\mu_b - k_{rb} - k_{db})A_b$ |

### *8.3.4 Nutrient and Interaction with Flow and Sediment Transport*

Surface runoff can remove large quantities of nutrients from the soil in both dissolved and particulate forms. The loss of dissolved nutrients in surface runoff is the result of rainfall mixing with the dissolved nutrients in the upper portion of the soil. Dissolved nutrients interact with surface runoff and once in water, they are transported. Suspended nutrients, which are assumed to be either organic or adsorbed inorganic components, attach to eroded sediment material derived from erosion, and are transported with water. The process of erosion is selective for finer particles. The finer particles, particularly clay, have larger surfaces of adsorption, and the clay fraction contains much of the organic matter and hydrous oxides (iron and aluminum) that can bind nitrogen and phosphorus (Nelson and Logan 1983). Runoff has two roles in the transport of nutrients: particle detachment and transport. Most of the nitrogen leaving watersheds through surface runoff is attached to finer soil particles. Novotny and Chester (1981) reported enrichment ratios for organic nitrogen or nitrogen adsorbed onto organic matter ranging from 2 to 4. Surface runoff also contains dissolved forms of nitrogen including $NH_4^+$ and $NO_3^-$. Phosphorus is most commonly assumed to be transported predominantly in particulate forms through soil erosion by surface runoff. Particulate phosphorus is attached to mineral and organic sediment as it moves with the runoff. The enrichment ratio for particulate phosphorus varies from 1 to 10 depending on watershed size and soil characteristics. However, where soil erosion is limited, the majority of phosphorus transported by surface runoff may be in dissolved forms.

#### 8.3.4.1 Dissolved Mass Transfer from the Upper Soil

The complicated nature of the flux at the soil or sediment surface is usually characterized through the use of a mass transfer coefficient, an empirical coefficient that relates the concentration gradient to mass transport (Choy and Reible 1999). The transfer rate of dissolved species from the soil to the water column is affected by the concentration gradient across the water-soil interface as well as flow conditions in the water column. This rate is computed with the NSM and then incorporated into the GSSHA-NSM integration as an external source/sink flux. Mass transfer theory states that the mass flux of a given species under a given set of flow conditions can be expressed as:

$$S_d = k_e(C_{d2}/\phi - C_d) \tag{8.10}$$

where $S_d$ is mass transfer flux of a dissolved species [$ML^{-2}T^{-1}$], $C_d$ is dissolved concentration of a species in the water column, $C_{d2}$ is dissolved concentration of a species in the soil layer in terms of mass of the substance per bulk volume of the soil layer [$M/L^3$], $k_e$ is mass transfer coefficient between water column and soil layer [L/T], and $\phi$ is porosity of the soil layer.

#### 8.3.4.2 Leaching

Nitrate is highly mobile as discussed previously and subject to leaching losses when both soil $NO_3^-$ content and water movement are high. $NO_3^-$ leaching from soils must be carefully controlled because of the serious impact that it can have on the groundwater. Movement of $NO_3^-$ through soil is governed by bulk flow which results in the movement of nitrate with the flow of water, molecular diffusion which results in the movement of nitrate due to the concentration gradient, and hydrodynamic dispersion in the soil due to the heterogeneity and internal structure of the soil. Leaching of $NH_4^+$ is usually insignificant.

Phosphorus is mainly bound to the fine soil particles. Only a small fraction of the phosphorus in the soil is present in the dissolved phase. However, some dissolved phosphorus is transported with runoff, and small amounts of phosphorus can reach the ground water through leaching. The amount of percolating phosphorus is controlled by the phosphorus adsorptive capacity of the soils above the aquifer (Nelson and Logan 1983). Transport of dissolved phosphorus involves the same processes as those described for N: convection, diffusion and hydrodynamic dispersion. These flux terms are computed through the GSSHA-NSM integration.

#### 8.3.4.3 Erosion and Sedimentation

The erosion and sedimentation of sediments and associated pollutants are two important processes in water quality modeling. Sediment detachment by surface

runoff is usually simulated in terms of a generalized erosion-deposition theory proposed by Smith et al. (1995). This assumes that the transport capacity concentration of the runoff reflects a balance between the two continuous counteracting processes of erosion and deposition. In general, the insoluble forms of nitrogen and phosphorus far exceed their soluble forms, the physical transport rate of both inorganic and organic forms of nitrogen and phosphorus with sediment is computed through NSM integration with GSSHA. The transport of nutrient particulates from the soil surface to the water column via erosion occurs at a rate that is proportional to the rate at which sediment particles are eroded (resuspended).

$$S_r = \sum_{n=1}^{N} f_p^n v_r^n C_{s2}^n \tag{8.11}$$

where $S_r$ is total erosion rate of a nutrient [$ML^{-2}T^{-1}$], $C_{s2}^n$ is particulate concentration associated with particle "$n$" in the soil layer [$M/L^3$], $f_p^n$ is fraction of the total chemical in the sorbed phase associated with particle "$n$", and $v_r^n$ can be defined as a erosion velocity associated with particle "$n$" [L/T].

The magnitude of the deposition flux of a contaminant is equal to the product of the rate of sediment deposition and the contaminant concentration associated with the settling particles. Settling velocity depends not only on the size, shape, and density of particles, but also on the concentration of the particles. The deposition of particulate nutrients from the water column is computed as:

$$S_s = \sum_{n=1}^{N} f_p^n v_s^n C_s^n \tag{8.12}$$

where $S_s$ is total deposition rate of a nutrient [$ML^{-2}T^{-1}$], $C_s^n$ is particulate concentration associated with particle "$n$" in water column [$M/L^3$], and $v_s^n$ is settling velocity associated with particle "$n$" [L/T].

## 8.4 Water Flow, Sediment and Nutrient Modeling Validation

Model validation is important in verifying that the proper processes are represented adequately. Currently there are two case studies underway to validate the nutrient cycling processes at Eau Galle Watershed. The Eau Galle Watershed encompasses a 402 $km^2$ area in northwest Wisconsin, Fig. 8.4. The lower portion of the watershed is relatively data poor. The upper portion of the watershed, that portion above Spring Valley Dam, has been the subject of intensive past studies, and is relatively data rich. In addition to the concern about agricultural effects on water quality in the lake and river, there are concerns about the effects of land use change on hydrologic and water quality conditions in the larger Eau Galle River system. Hydrology, sediment transport, nutrient cycling and export were examined

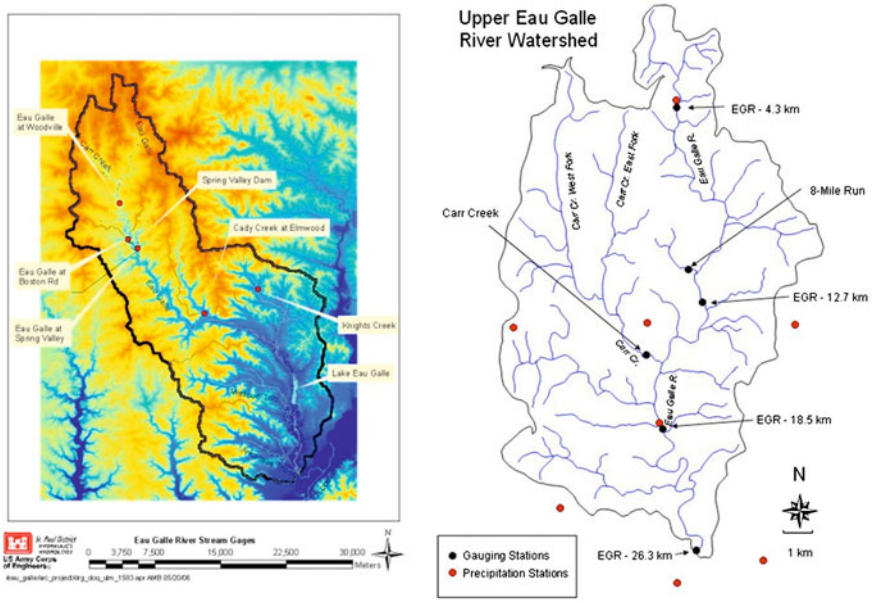


**Fig. 8.4** Eau Galle River watershed and sampling locations

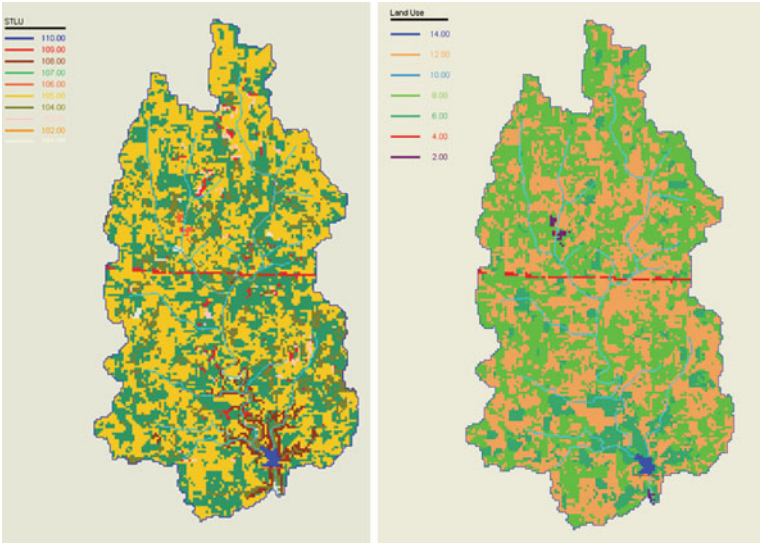


**Fig. 8.5** Eau Galle River watershed land use and soil distribution

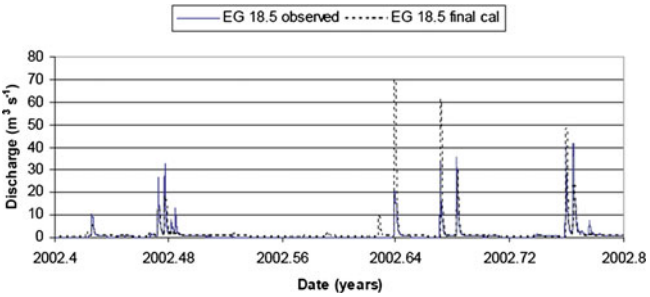


**Fig. 8.6** Calibrated and observed flow discharge at EG 8.5

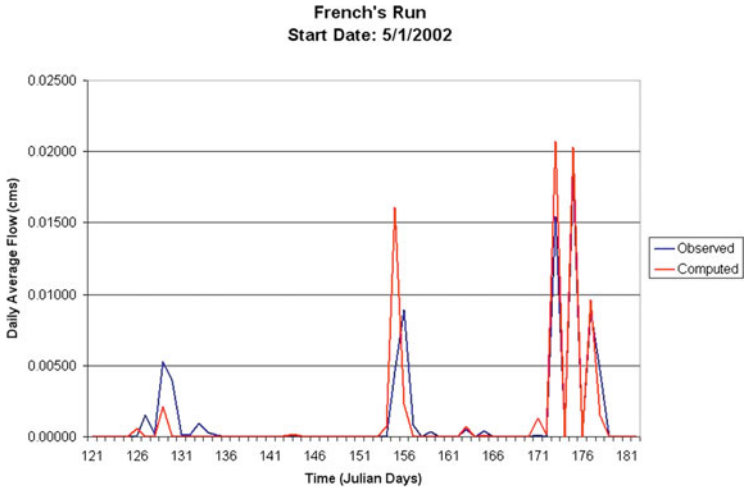


**Fig. 8.7** Calibrated and observed flow discharge at Franch's Run

at the Upper Eau Galle River watershed and at one sub-watershed at an adjacent watershed (French Creek).

The land use and soil type maps are shown in Fig. 8.5a and b, respectively. The land uses includes residential, commercial, forest, grass, wetland, row crop, and open water. The predominate land uses in the watershed are pasture (8, light green) and row crops (12, beige). There is a moderate amount of forest (6, dark green), with limited residential and commercial use. The predominant soil type is silty loam.

The hydrologic model of GSSHA was developed and calibrated to observed flows at the USGS gauge (EG 8.5 in Fig. 8.4) because this site was believed to provide the most reliable data for model calibration. Flows from the other sites are considered less reliable. Results of the model calibration during the period June through October 2002 are shown in Fig. 8.6. The mean absolute error (MAE) of

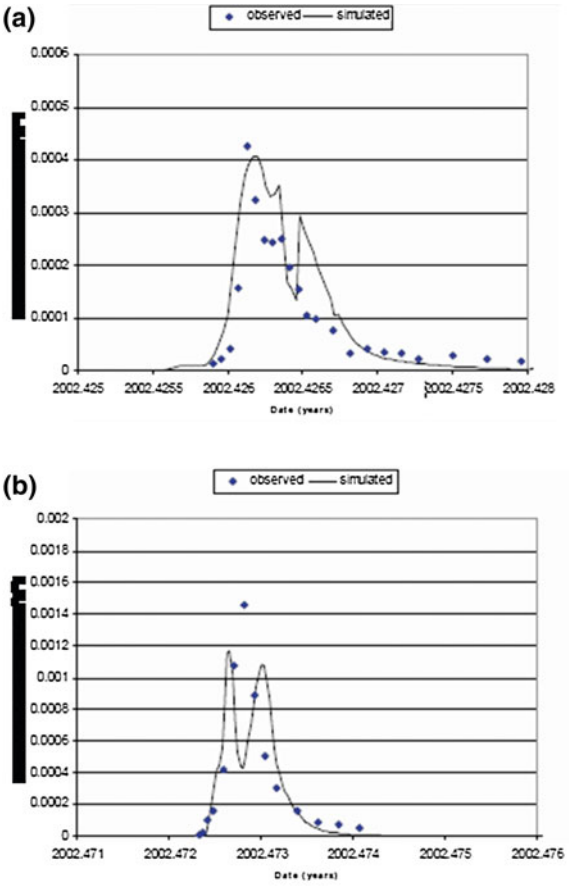


**Fig. 8.8** Calibrated and observed total suspended sediment at EG 8.5

the larger two peaks is 3 percent of the observed. The error in total discharge is 1.5 percent of observed. The hydrograph shapes and base flow are accurately reproduced. The GSSHA model was able to adequately simulate hydrology as seen by the above calibration.

The French's Run study site was located in the headwaters of French Creek watershed, which is adjacent to and just south of the Upper Eau Galle River basin. The only defined channels in French's Run were ditches located on either side of two roads that bisected the watershed. Land use in the watershed was dominated by corn production during the study period and flows during storm events occurred as overland runoff from the field that drained directly into the ditches and a culvert that passed under a road. Runoff was exacerbated by contouring crop rows parallel to the slope of the field to promote better field drainage (James et al. 2003). Calibrated and observed flow discharge at French's run gage is given in Fig. 8.7.

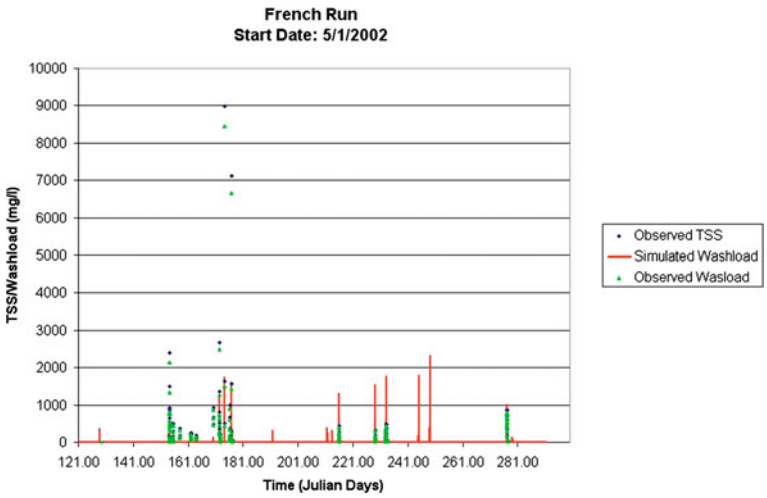


**Fig. 8.9** Calibrated and observed total suspended sediment at Franch's Run

Three sediment size fractions were simulated, sand, silt, and clay. The model was calibrated to two observed events that occurred in June 2002 using the hydrologic parameters from calibration 1. Observed values of total suspended solids (TSS) and flow were combined according to USGS standards to produce sediment discharge ($m^3\ s^{-1}$) and compared to the model stream values of wash load, which is composed of clay and silt size fractions. The sand is expected and assumed to move as bed load and not be in TSS measurements. The calibration results are shown in Fig. 8.8. The MAE for the total sediment discharge ($m^3$) for the two events was 12 and 4 percent of the observed, respectively. In general, the sediment calibration and verification results are good.

For the field scale, calibrated and observed suspended sediment at French's run gage is given in Fig. 8.9.

The nutrient cycling simulation within GSSHA was tested and validated for the same watershed. In preparing the nutrient loadings, total nitrogen and total phosphorous were measured, and the soluble forms were estimated from these totals as inputs. No continuously N and P concentration measurement data were available. The model calibration for water quality was conducted only for dissolved N and P at gages where observed data were available. Based on multiple GSSHA runs, Fig. 8.10 shows the comparison between observed and modeled nitrate N and dissolved inorganic P for the same simulation period with the hydrology. The figure indicates that the trend of modeled nutrient concentration match with the trend of the measured data.

For the field scale, calibrated and observed flow inorganic phosphorus at French's run gage is given in Fig. 8.11.

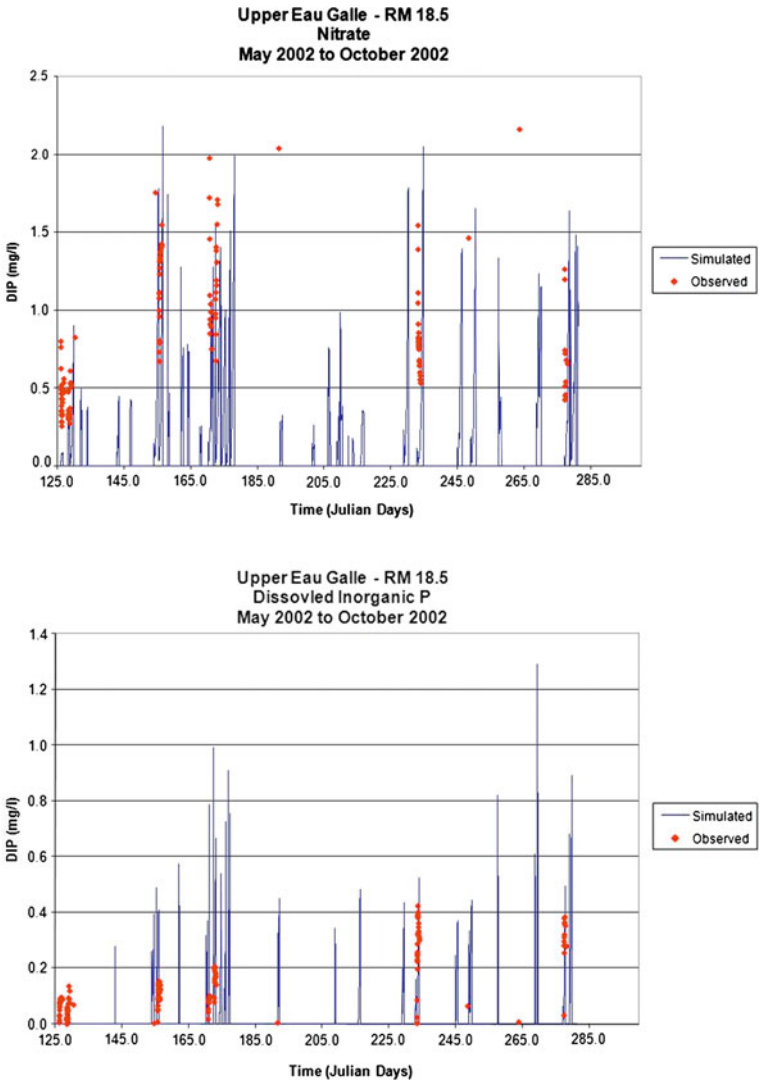


**Fig. 8.10** Modeled and observed nitrogen and phosphorus results at EG 8.5

As the results of the demonstrative application show, the model presently developed achieves detailed analysis of the water quality aspects of a watershed including nutrient transport and fate across the landscape. Due to limited data issues it is inferred that current GSSHA modeling system needs further testing and validation at the watershed scale.

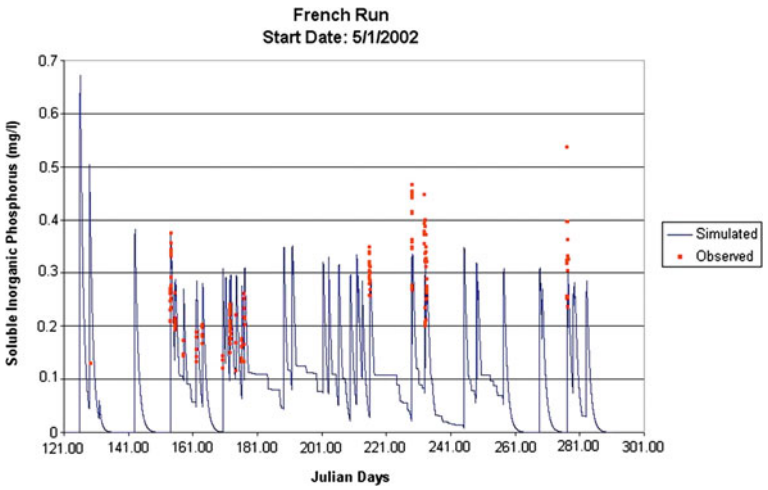


**Fig. 8.11** Modeled and observed inorganic phosphorus results at Franch's Run

## 8.5 Summary

The GSSHA model has the capability to simulate hydrology, hydraulics, and sediment transport in variety of watershed applications. A distributed nutrient transport and transformation modeling has been integrated with GSSHA. The nutrient modeling described in this chapter is able to simulate both soil, surface runoff and channel processes of nitrogen and phosphorus cycling. Now the model is composed of cascade-linked three sub-models. An integrated model serves to evaluate evapotranspiration, infiltration, soil water content, discharge, soil erosion, nutrient transport and fate. The GSSHA was applied to a real watershed—upstream of the Spring Valley Dam located on the Eau Galle River in Wisconsin. The GSSHA model was able to adequately simulate hydrology and sediment transport as seen by the calibration. The model closely reproduces discharge and sediment transport during the calibration. This application also demonstrated its capabilities in simulating the fate and transport of nutrients in watersheds as well. The ability to simulate spatially distributed nutrient concentrations within the watershed has not been evaluated due to a lack of field data at this time.

Use of the structured grid in space is a great convenience in preparation of the input data including maps of soil texture, land use and nutrient loading. The GSSHA model generates time series outputs of model state variables at specified points in space over time. The model also provides the temporal variation and spatial distribution of sediment and nutrient transport. The GSSHA model is capable of predicting runoff depth, soil moistures, discharge, soil erosion, sediment and nutrient (nitrogen and phosphorus) transport and fate. The model is useful in determining the relative contributions of various sources of surface runoff and base flow and corresponding sediment and nutrient sources. Furthermore, the GSSHA

model has the advantage of being fully distributed and physically based. All simulation parameters employed have physical or well-established empirical meaning, and all are within the bounds of published or field measured values. It is thus concluded that the model could be a powerful tool to investigate and assess the time-varying hydrology and sediment and nutrient transport and fate of a watershed. Especially, in agricultural sector, it would absolutely be an invaluable tool for quantifying water quality impacts by agricultural farming and practices. However, model physically based formulation will require application on a data set that includes detailed rainfall, soil moisture, and distributed source observations.

## Appendix: Water Quality Parameters

| | |
|---|---|
| $orgN_{frs}$ | concentration of soil layer fresh organic N pool [M/L$^3$] |
| $ON_{min\|imb}$ | net mineralization/immobilization rate of soil layer fresh organic N pool [M/L$^2$/T] |
| $ON_{dec}$ | decomposition rate of soil layer fresh organic N pool [M/L$^2$/T] |
| $ON_{frs,e}$ | net surface erosion/deposition rate of soil layer fresh organic N pool [M/L$^2$/T] |
| $ON_{frs,s}$ | external sources [M/L$^2$/T] |
| $orgN_{act}$ | concentration of soil layer active organic N pool [M/L$^3$] |
| $ON_{trn}$ | rate transferred between the active and stable organic N pools [M/L$^2$/T] |
| $ON_{min}$ | mineralization rate of soil layer active organic N pool [M/L$^2$/T] |
| $ON_{act,e}$ | net surface erosion/deposition rate of soil layer active organic N pool [M/L$^2$/T] |
| $ON_{act,s}$ | external sources [M/L$^2$/T] |
| $ON_{sta,e}$ | net surface erosion/deposition rate of soil layer stable organic N pool [M/L$^2$/T] |
| $ON_{sta,s}$ | external sources added to the soil layer stable organic N pool [M/L$^2$/T] |
| $NH_4^+$ | concentration of soil layer $NH_4^+$ pool [M/L$^3$] |
| $NH_{min}$ | total mineralization processes rate of soil layer organic N pools [M/L$^2$/T] |
| $NH_{nit\|vol}$ | net nitrification/volatilization processes rate in the soil layer [M/L$^2$/T] |
| $NH_{up}$ | plant uptake rate of soil layer $NH_4^+$ pool [M/L$^2$/T] |
| $R_{NH4,e}$ | mass transfer rate of $NH_4^+$ between the upper soil layer and surface runoff [M/L$^2$/T] |
| $NH_s$ | external sources [M/L$^2$/T] |
| $NO_3^-$ | concentration of soil layer $NO_3^-$ pool [M/L$^3$] |
| $NO_{dnit}$ | denitrification processes rate in the soil layer [M/L$^2$/T] |
| $NO_{up}$ | plant uptake rate of soil layer $NO_3^-$ pool [M/L$^2$/T] |

$R_{NO3,e}$ mass transfer rate of $NO_3^-$ between the upper soil layer and surface runoff [M/L$^2$/T]
$R_{NO3,f}$ infiltration rate of soil layer $NO_3^-$ pool [M/L$^2$/T]
$NO_s$ external sources [M/L$^2$/T]
$PON_{ov}$ concentration of the overland flow PON [M/L$^3$]
$orgN$ total concentration of organic N in the upper soil layer [M/L$^3$]
$k_{hn}$ PON hydrolysis rate constant [1/T]
$DON_{ov}$ concentration of DON in the overland flow [M/L$^3$]
$k_{mn}$ DON mineralization rate constant [1/T]
$NH_{4\,ov}^+$ concentration of $NH_4^+$ in the overland flow [M/L$^3$]
$k_{en}$ effective mass transfer rate constant [L/T]
$k_{nit}$ nitrification rate constant [1/T]
$R_{NH4,up}$ plant uptake rate of the overland flow $NH_4^+$ [M/L$^3$/T]
$NO_{3\,ov}^-$ concentration of $NO_3^-$ in the overland flow [M/L$^3$]
$R_{NO3,up}$ plant uptake rate of the overland flow $NO_3^-$ [M/L$^3$/T]
$orgP_{frs}$ concentration of soil layer fresh organic P pool [M/L$^3$]
$OP_{dec}$ decomposition rate of soil layer fresh organic P pool [M/L$^2$/T]
$OP_{min|imb}$ net mineralization/immobilization rate of soil layer fresh organic P pool [M/L$^2$/T]
$OP_{frs,e}$ net surface erosion/deposition rate of soil fresh organic P pool [M/L$^2$/T]
$OP_{frs,s}$ external sources [M/L$^2$/T]
$orgP_{act}$ concentration of soil layer active organic P pool [M/L$^3$]
$OP_{min}$ mineralization rate of soil humic active organic P pool [M/L$^2$/T]
$OP_{trn}$ rate transferred between the active and stable organic P pools [M/L$^2$/T]
$OP_{act,e}$ net surface erosion/deposition rate of soil humic active organic P pool [M/L$^2$/T]
$OP_{act,s}$ external sources [M/L$^2$/T]
$orgP_{sta}$ concentration of soil layer stable organic P pool [M/L$^3$]
$OP_{sta,e}$ net surface erosion/deposition rate of soil humic stable organic P pool [M/L$^2$/T]
$OP_{sta,s}$ external sources [M/L$^2$/T]
$P_{sol}$ concentration of soil layer soluble P pool [M/L$^3$]
$IP_{min}$ total mineralization processes rate of soil layer organic P pools [M/L$^2$/T]
$IP_{sol|act}$ net sorption rate transferred between the soluble P pool and active inorganic P pool [M/L$^2$/T]
$IP_{up}$ plant uptake rate of soil layer soluble P pool [M/L$^2$/T]
$R_{DIP,e}$ mass transfer rate of soluble P between the upper soil layer and surface runoff [M/L$^2$/T]
$IP_s$ external sources [M/L$^2$/T]
$minP_{act}$ concentration of soil layer active inorganic P pool [M/L$^3$]

$IP_{act|sta}$ net slow sorption transfer rate between the active inorganic P pool and the stable inorganic P pool [M/L$^2$/T]
$IP_{act,e}$ surface erosion/deposition rate of soil active inorganic P detachment [M/L$^2$/T]
$IP_{act,s}$ external sources [M/L$^2$/T]
$minP_{sta}$ concentration of soil layer stable inorganic P [M/L$^3$]
$IP_{sta,e}$ surface erosion/deposition rate of soil stable inorganic P detachment [M/L$^2$/T]
$IP_{sta,s}$ external sources [M/L$^2$/T]
$POP_{ov}$ concentration of POP in the overland flow [M/L$^3$]
$orgP$ total concentration of organic P in the upper soil layer [M/L$^3$]
$k_{hp}$ POP hydrolysis rate constant [1/T]
$DOP_{ov}$ concentration of DOP in the overland flow [M/L$^3$]
$k_{mp}$ DOP mineralization rate constant [1/T]
$DIP_{ov}$ concentration of DIP in the overland flow [M/L$^3$]
$k_{ep}$ DIP mass transfer rate between the upper soil layer and overland flow [L/T]
$R_{DIP,up}$ plant uptake rate of the overland flow DIP [M/L$^3$/T]
$PON_{ch}$ concentration of in-stream PON [M/L$^3$]
$k_{dp}$ temperature-dependent phytoplankton death rate [T$^{-1}$]
$k_{db}$ temperature-dependent bottom algae death rate [T$^{-1}$]
$A_p$ stream phytoplankton concentration [M/L$^3$]
$A_b$ stream bottom algae concentration [M/L$^2$]
$k_{hn}$ temperature-dependent PON hydrolysis rate coefficient [T$^{-1}$]
$DON_{ch}$ concentration of in-stream DON [M/L$^3$]
$k_{mn}$ temperature-dependent DON mineralization rate coefficient [T$^{-1}$]
$F_{oxmn}$ DON mineralization attenuation due to low oxygen
$TNH_{4\,ch}^{+}$ Total concentration of in-stream $NH_4^+$ [M/L$^3$]
$k_{rp}$ temperature-dependent phytoplankton respiration rate [T$^{-1}$]
$F_{oxna}$ nitrification attenuation due to low oxygen
$k_{nit}$ temperature-dependent $NH_4^+$ nitrification rate coefficient [T$^{-1}$]
$P_{ap}$ preference coefficient of phytoplankton for $NH_4^+$
$P_{ab}$ preference coefficient of bottom algae for $NH_4^+$
$NO_{3\,ch}^{-}$ concentration of in-stream $NO_3^-$ [M/L$^3$]
$K_{scdn}$ DOC half-saturation constant for denitrification [gC/m$^3$] [M/L$^3$]
$k_{dnit}$ temperature-dependent $NO_3^-$ denitrification rate coefficient [T$^{-1}$]
$F_{oxdn}$ effect of low oxygen on denitrification
$POP_{ch}$ concentration of in-stream POP [M/L$^3$]
$DOP_{ch}$ concentration of in-stream DOP [M/L$^3$]
$TIP_{ch}$ total concentration of in-stream inorganic P [M/L$^3$]
$k_{hp}$ temperature-dependent POP hydrolysis rate coefficient [T$^{-1}$]
$k_{mp}$ temperature-dependent DOP mineralization rate coefficient [T$^{-1}$]
$F_{oxmp}$ DOP mineralization attenuation due to low oxygen
$POC_{ch}$ concentration of in-stream POC [M/L$^3$]

| | |
|---|---|
| $DOC_{ch}$ | concentration of in-stream DOC [M/L$^3$] |
| $DIC_{ch}$ | concentration of in-stream DIC (mole/L) [M/L$^3$] |
| $k_{hc}$ | temperature-dependent POC hydrolysis rate coefficient [T$^{-1}$] |
| $F_{oxmc}$ | DOC mineralization attenuation due to low oxygen |
| $k_{mc}$ | temperature-dependent DOC mineralization rate [T$^{-1}$] |
| $k_{ac}$ | 0.923 $k_a$ = temperature-dependent $CO_2$ deaeration coefficient [T$^{-1}$] |
| $k_H$ | Henry's constant [mole/(L atm)] |
| $p_{CO2}$ | partial pressure of carbon dioxide in the atmosphere [atm] |
| $\alpha_0$ | fraction of total inorganic carbon in carbon dioxide |
| $DO_{ch}$ | concentration of in-stream DO [M/L$^3$] |
| $k_a$ | temperature-dependent oxygen reaeration coefficient [T$^{-1}$] |
| $DO_s$ | saturation concentration of oxygen [mg$O_2$/L] |
| $S_{SOD}$ | sediment oxygen demand rate [M/L$^3$] |
| $A_b$ | stream bottom algal concentration [M/L$^2$] |
| $\mu_b$ | benthic algal photosynthesis rate [T$^{-1}$] |
| $F_{oxb}$ | attenuation due to low oxygen |
| $k_{rb}$ | temperature-dependent benthic algal respiration rate [T$^{-1}$] |
| $k_{db}$ | temperature-dependent benthic algal death rate [T$^{-1}$] |

## References

Beuselinck L, Govers G, Steegen A, Quine TA. Sediment transport by overland flow over an area of net deposition. Hydrol Process. 1999;13(17):2769–82.

Burban PY, Xu Y, McNeil J, Lick W. Settling speeds of flocs in fresh and sea waters. J Geophys Res [Oceans]. 1990;95(C10):18213–20.

Burt TP, Haycock NE. Controlling losses of nitrate by changing land use. In: Burt TP, Heathwaite AL, Trudgill ST, editors. Nitrate: processes, patterns and management. Wiley; 1993. p. 342–67.

Cheng NS. Simplified settling velocity formula for sediment particle. J Hydraul Eng. 1997;123(2):149–152

Choy B, Reible DD. Contaminant transport in soils and sediments: mathematic analysis. Report to the Hazardous Substance Research Center (S&SW), Baton Rouge: Louisiana State University; 1999.

Coastal and Hydraulic Laboratory (CHL). http://chl.erdc.usace.army.mil/gssha 2012.

Downer CW, Ogden FL. GSSHA: a model for simulating diverse streamflow generating processes. J Hydrol Eng. 2004;9(3):161–74.

Haralampides K, McCourquodale JA, Krishnappan BG. Deposition properties of fine sediment. J Hydraul Eng. 2003;129(3):230–4.

Holley ER. Unified view of diffusion and dispersion. J Hydraul Div. 1969;95(2):621–31.

James WF, Eakin HL, Barko JW. Phosphorus forms and export from sub-watersheds in the Upper Eau Galle River basin exhibiting differing land-use practices. Water Quality Technical Notes Collection (ERDC WQTN-PD-15), US. Vicksburg: Army Engineer Research and Development Center; 2003.

Julien PY, Simons DB. Sediment transport capacity of overland flow. Trans ASAE. 1985;28:755–62.

Julien PY, Saghafian B, Ogden FL. Raster-based hydrologic modeling of spatially-varied surface runoff. Water Resour Bull. 1995;31(3):523–36.

Julien PY. Erosion and sedimentation. Cambridge: Cambridge University Press; 1998.
Krishnappan BG. In situ distribution of suspended particles in the Frasier River. J Hydraul Eng. 2000;126(8):561–9.
Nelson DW, Logan TJ. Chemical processes and transport of phosphorus. In: Schaller FW, Bailey GW, editors. Agricultural management and water quality. Iowa State University Press; 1983. p. 65–91.
Novotny V, Chester G. Handbook of nonpoint pollution: sources and management. New York: Van Nostrand Reinhold Co.; 1981.
Simons DB, Sentürk F. Sediment transport technology: water and sediment dynamics (revised edition). Littleton: Water Resources Publications; 1992.
Smith RE, Goodrich D, Quinton JN. Dynamic distributed simulation of watershed erosion: the KINEROS2 and EUROSEM models. J Soil Water Conserv. 1995;50:517–20.
USEPA (US Environmental Protection Agency). Hypoxia in the Northern Gulf of Mexico: an update by the EPA Science Advisory Board, EPA-SAB-08-003; 2007.